Preclinical Pharmacokinetics of Ranibizumab (rhuFabV2) after a Single Intravitreal Administration

Jacques Gaudreault,[1] David Fei,[2] Jeriza Rusit,[3] Pamela Suboc,[2] and Vanessa Shiu[1]

Purpose. Ranibizumab (rhuFab V2; Lucentis, Genentech, South San Francisco, CA) is a humanized monoclonal antibody fragment designed to bind all forms of VEGF, thereby blocking vessel permeability and angiogenesis in neovascular age-related macular degeneration. This study evaluated the pharmacokinetic (PK) and serum bioavailability of ranibizumab after a single intravitreal (ITV) or intravenous (IV) dose in cynomolgus monkeys.

Methods. Monkeys received ranibizumab as either a bilateral ITV dose (500 or 2000 μg/eye; $n = 6$/group) or a single IV dose (1000 or 4000 μg/animal; $n = 4$/group). After ITV administration, ranibizumab concentrations were measured in several ocular compartments and in serum for 10 days and, after IV administration, for 48 hours. Pharmacokinetic parameters were estimated by compartmental and noncompartmental methods.

Results. Ranibizumab cleared in parallel from all ocular compartments, with a terminal half-life of approximately 3 days. It distributed rapidly to the retina (6–24 hours), and concentrations were approximately one third that in the vitreous. After ITV injection, bioavailability (F) was 50% to 60%. Serum concentrations were very low, reflecting wider distribution and faster clearance when ranibizumab reached the serum. After IV administration, the terminal half-life was approximately 0.5 day.

Conclusions. This study demonstrates that ranibizumab has a PK profile that is favorable for its clinical use in treating neovascular AMD by monthly ITV injection. (*Invest Ophthalmol Vis Sci.* 2005;46:726–733) DOI:10.1167/iovs.04-0601

Age-related macular degeneration (AMD) is the most common cause of blindness in older adults in the Western world[1,2] and is classified into two forms[3]: nonexudative (dry) and neovascular exudative (wet). Although the neovascular form represents 20% of all cases, it accounts for approximately 80% to 90% of severe vision loss.[4]

Although the pathogenesis of neovascular AMD has not been completely elucidated, considerable evidence indicates that vascular endothelial growth factor (VEGF) plays an important role, by inducing both angiogenesis and microvascular leakage. Preclinical and clinical findings strongly support VEGF involvement in AMD, including VEGF expression in choroidal neovascular membranes of patients with AMD,[5,6] VEGF-induced neovascularization in primate eyes (Cui JZ, et al. *IOVS* 1997;38:ARVO Abstract 1670),[4] reduced neovascularization and vessel permeability after VEGF inhibition in a primate model of corneal neovascularization (CNV),[7] and increased retinal and vitreous VEGF levels in patients and animals with ischemic retinopathies.[8–11]

To date, several forms of VEGF have been identified, most produced by alternative splicing ($VEGF_{121}$, $VEGF_{145}$, $VEGF_{165}$, $VEGF_{183}$, $VEGF_{189}$, and $VEGF_{206}$), and $VEGF_{110}$, produced by plasmin cleavage of the six isoforms.[12] Although the role that each form plays in AMD remains unclear, retinal expression of both $VEGF_{121}$ and $VEGF_{165}$ has been documented in normal eyes of rats, monkeys, and humans.[13–17]

Ranibizumab (rhuFabV2, Lucentis; Genentech, South San Francisco, CA), a humanized monoclonal antibody fragment, is designed to bind all isoforms of VEGF and block vessel permeability and angiogenesis. It binds and inhibits $VEGF_{165}$, $VEGF_{121}$, and $VEGF_{110}$ (Lowe J, et al. *IOVS* 2003;44:ARVO E-Abstract 1828) and has also been shown to penetrate all layers of the rabbit retina—the first demonstration of retinal penetration of an anti-VEGF therapy intended for AMD.[18] This ability has been attributed to the small molecule size (48 kDa), because a full-length antibody (trastuzumab, 148 kDa) was not able to penetrate all the retinal layers of rhesus monkeys.[19] The small molecular radius of ranibizumab probably also contributes to its demonstrated ability to penetrate the retina. Although intrascleral administration could be considered, because of the small size of ranibizumab, intravitreal injection was selected to maximize the VEGF inhibitory effect in the retina, while limiting systemic VEGF inhibition.[19] Thus, ITV administration should minimize interference with the normal extraocular roles of VEGF.[20]

The objective of this study was to investigate the systemic (serum), vitreous, aqueous humor, and retinal pharmacokinetics (PK) of ranibizumab, when administered as a single ITV injection to monkeys, and to determine the systemic bioavailability (F) after ITV and intravenous (IV) administration.

Materials and Methods

Study Design

The study was conducted according to the ARVO Statement for the Use of Animals in Ophthalmic and Vision Research. Cynomolgus monkeys received either a single bilateral ITV dose of ranibizumab or a single IV bolus dose. The eyes and serum samples were collected and analyzed for drug concentration and for anti-ranibizumab antibody, for up to 10 days after administration.

Drug Administration and Sampling

Ten male and 10 female monkeys, 2.2 to 4.5 kg on the day before drug administration, were assigned to four groups ($n = 6$ in groups 1 and 2; $n = 4$ in groups 3 and 4; Table 1). Group-1 and -2 animals received a single bilateral ranibizumab ITV dose of 500 or 2000 μg/eye, respectively (1000 or 4000 μg/animal), through a 30-gauge needle. Animals were sedated (10 mg/kg ketamine HCl, 0.5 mg/kg diazepam) and treated with topical proparacaine. Ranibizumab was then administered

From the Departments of [1]Pharmacokinetic and Pharmacodynamic Sciences, [2]Bioanalytical Research and Development, and [3]Bio-Analytical Assays, Genentech, Inc., South San Francisco, California.

Supported by Genentech, Inc.

Submitted for publication May 26, 2004; revised September 9 and October 27, 2004; accepted November 3, 2004.

Disclosure: **J. Gaudreault**, Genentech, Inc. (E, F); **D. Fei**, Genentech, Inc. (E, F); **J. Rusit**, Genentech, Inc. (E, F); **P. Suboc**, Genentech, Inc. (E, F); **V. Shiu**, Genentech, Inc. (E, F)

The publication costs of this article were defrayed in part by page charge payment. This article must therefore be marked "*advertisement*" in accordance with 18 U.S.C. §1734 solely to indicate this fact.

Corresponding author: Jacques Gaudreault, Pharmacokinetic and Pharmacodynamic Sciences, Genentech, Inc., 1 DNA Way, South San Francisco, CA 94080; jacques@gene.com.

Investigative Ophthalmology & Visual Science, February 2005, Vol. 46, No. 2
Copyright © Association for Research in Vision and Ophthalmology

Downloaded from iovs.arvojournals.org on 01/21/2024

Regeneron Ex. 2017
Fresenius v. Regeneron
IPR2025-01268
Page 1 of 8

TABLE 1. Treatment Groups Assignment

Group	Number per Group (M/F)	Route	Day Administered	Dose	Dose Concentrations (mg/mL)	Dose Volume
1	3/3	ITV	1	500 μg/eye	10	50 μL/eye
2	3/3	ITV	1	2000 μg/eye	40	50 μL/eye
3	2/2	IV	1	1000 μg/animal	1	1 mL
4	2/2	IV	1	4000 μg/animal	4	1 mL

through the sclera and pars plana, 4 mm posterior to the limbus, with the needle directed posterior to the lens into the midvitreous. Group-3 and -4 monkeys received a single IV bolus (1 mL) of drug at 1000 or 4000 μg/animal, respectively. Ranibizumab was formulated as 10 mM sodium succinate, 10% trehalose, and 0.05% Tween-20 (pH 5.0).

Ocular tissues were collected from groups 1 and 2. One animal per group was killed at the following times: days 1 (6 hours after the dose) 2, 3, 5, 8, and 11. At death, both eyes were enucleated, and ranibizumab concentrations were determined in the vitreous and aqueous humor and retinal tissues. Retinal tissues were separated into two layers—the neural retina (NR) and the retinal pigment epithelium/Bruch's membrane/choriocapillaris (RPE/Bruch's), under a magnifying device, with Ames solution used to facilitate layers separation. The entire layers were collected without isolating specific regions (e.g., the macula), and the ranibizumab concentrations represent the average for the entire layer. Layers were analyzed separately, and ranibizumab concentrations were also determined in the Ames solution used for dissection. Dissections were completed within 30 minutes of euthanasia.

All blood samples (approximately 1 mL) were collected via a femoral or cephalic vein. After ITV administration, samples were drawn before the dose and at 2, 6, 12, 24, 36, and 48 hours and daily from days 4 to 11 after the dose (samples drawn from all available animals at each time). After IV administration, samples were drawn at 5, 15, and 30 minutes; hourly from 1 to 10 hours; and at 16, 24, 36, and 48 hours after the dose. For analysis of anti-ranibizumab antibodies, blood samples were collected from available animals at screening, before administration on day 1, and after on days 5, 8, and 11. Samples were also collected from group-3 and -4 animals on days 15 and 30. Within 1 hour of blood collection, samples were clotted at room temperature, and serum was separated by centrifugation and stored at −60°C to −80°C.

Measurements and Evaluations

Animals were observed twice daily for signs of potential adverse events, and once daily for qualitative assessment of food consumption. Body weight was determined before administration and at necropsy for groups 1 and 2. Ophthalmic evaluations on ITV-group animals were conducted once during the screening period, before the dose and on days 2, 8, and 11 after drug administration.

Ranibizumab concentrations in the ocular compartments, serum, and Ames solution were determined by a validated enzyme-linked immunosorbent assay (ELISA) developed at Genentech, Inc., using recombinant human $VEGF_{165}$ for capture and a goat anti-human $F(ab')_2$ fragment conjugated with horseradish peroxidase (HRP) for detection. Assay performance is summarized in Table 2. VEGF concentrations in the ocular compartments were determined by a fluorometric bridging ELISA, with a monoclonal mouse antibody to rhVEGF (3.5F8) used for capture and the same antibody, conjugated with biotin, for detection. This assay measures free VEGF and ranibizumab-bound VEGF. The minimum quantifiable concentration of VEGF in the vitreous and aqueous humors was ≤20 pg/mL and ≤0.02 pg/mg of retina dry weight. Assay accuracy ranged from 90% to 109% (n = 16) with intra- and interassay coefficients of variation ranging between 11% and 26% and 12% and 28%, respectively. Serum antibodies against ranibizumab were measured with a sandwich ELISA, using ranibizumab as the capturing agent and protein A/G conjugated with HRP for detection. Samples were screened at 1:100 dilution. Samples above the cutoff point, based on a pool of naïve monkey serum, were then titered. Titers <2.0 log titer units were considered negative.

Pharmacokinetic Analysis

Ranibizumab concentrations in the vitreous and aqueous humor and retinal layers were analyzed with a naïve-pooled approach. Total ranibizumab in the retina (the sum of the amount detected in the retinal layers and the Ames solution) was calculated and then divided by the net dry weight (in milligrams) of the NR and RPE/Bruch's layers. The resultant retinal ranibizumab concentrations, reported as nanograms per milligrams, were used for analyses. Vitreous parameters, after ITV administration, were determined with a one-compartment model, using individual concentrations. This analysis method assumes that ranibizumab clears from the eye monoexponentially. The pharmacokinetics of ranibizumab in aqueous humor, retina, and serum after ITV administration were determined by a noncompartmental method, using mean concentrations. Areas under the curve (AUC) were estimated by a linear-trapezoidal method, and the terminal half-life ($t_{½}$) was estimated by linear regression, using at least three concentration time points. In comparison to the compartmental method, the noncompartmental method does not require any assumption on the shape of the curve (i.e., mono- or multiexponential decline). All analyses were performed using WinNonlin Pro, ver. 1.5 (Pharsight Corp., Mountain View, CA).

Ranibizumab serum pharmacokinetics after IV administration were determined with a two-compartment model, because the concentration–time profiles declined rapidly at the beginning and more slowly thereafter (biexponential profile). $AUC_{(0-2d)}$ was determined for individual animals by using the linear-trapezoidal method. After ITV injection, drug bioavailability (F) was estimated by using the $AUC_{(0-2d,\ ITV)}/AUC_{(0-2d,\ IV)}$ ratio, because day 2 was the last time point when ranibizumab was detected after IV administration. Values below the sensitivity limit of the assays were excluded from all analyses and displays.

RESULTS

General Health and Clinical Findings

Ranibizumab was well tolerated. No clinical signs or changes in food consumption or body weight attributable to the drug were observed. After ITV administration, transient ocular inflammation, primarily vitreous cloudiness, ranged from absent to moderate (500 μg/eye) and moderate to severe (2000 μg/

TABLE 2. Ranibizumab ELISA Performance

Matrix	LLOQ (ng/mL)	Assay Range (ng/mL)	Accuracy (%)
Serum	15.6	0.156–5.00	88–114
Vitreous humor	1.56	0.156–5.00	99–109
Aqueous humor	1.56	0.156–5.00	N/A
Retina	0.78	0.156–5.00	83–99
Ames solution	15.6	0.156–5.00	85–111

LLOQ, lower limit of quantitation.

Downloaded from iovs.arvojournals.org on 01/21/2024

Regeneron Ex. 2017
Fresenius v. Regeneron
IPR2025-01268
Page 2 of 8

TABLE 3. Ranibizumab Ocular Pharmacokinetics after ITV Administration

	Vitreous		Aqueous Humor		Retina*	
	Group 1†	Group 2†	Group 1†‡	Group 2†‡	Group 1†‡	Group 2†‡
C_{max} (μg/mL)	169‡	612‡	116	478	78.6	227
t_{max} (d)	0.25‡	1‡	0.25	1	0.25	1
Terminal $t_{½}$ (day)	2.63§	3.95§	2.54	2.63	2.60	2.28
CL (mL/d)	0.671§	0.517§	—	—	—	—
V_c (mL)	2.55§	2.95§	—	—	—	—
MRT (d)	3.80§	5.69§	3.17	3.66	3.26	3.51
$AUC_{(0-t)}$ (d · μg/mL)	689‡	3110‡	231	1500	221	866
$AUC_{(0-\infty)}$ (d · μg/mL)	727‡	3300‡	242	1560	236	909

C_{max}, observed maximum concentration; t_{max}, time to C_{max}; CL, clearance; V_c, central volume of distribution; MRT, mean residence time; $AUC_{(0-t)}$, area under the curve until the last measurable concentration (~10 days); and $AUC_{(0-\infty)}$, area under the curve from 0 to infinity.

* Ranibizumab concentrations in the retina determined as nanograms per milligram of tissue, which is equivalent to micrograms per milliliter.

† Group 1 received ranibizumab, 500 μg/eye; group 2, ranibizumab 2000 μg/eye.

‡ Determined using a noncompartmental method.

§ Determined using a one-compartment model.

eye). The inflammation was present at day 2 but had completely resolved by day 8.

Ranibizumab Ocular Pharmacokinetics after ITV Administration

In group 1, ranibizumab peak vitreous concentration (C_{max}) was 169 μg/mL 6 hours after ITV administration (t_{max}; Table 3). In group 2, C_{max} was 3.6-fold higher (612 μg/mL), and t_{max} was 24 hours. Ranibizumab concentrations in both groups declined with similar $t_{½}$ of 2.6 and 4.0 days for group 1 and 2, respectively (Fig. 1, Table 3), and comparable clearances (0.671 mL/d for group 1, 0.517 mL/d for group 2). Likewise, dose-adjusted AUCs, were similar in both groups, suggesting dose-linear vitreous pharmacokinetics.

The distribution of ranibizumab from the vitreous, either to the aqueous chamber or to the retina, was very rapid (Table 3). In both the retina and the aqueous chamber, t_{max} was 6 hours and 1 day in groups 1 and 2, respectively. Ranibizumab terminal $t_{½}$ in the aqueous and the retina was 2.3 to 2.6 days, similar to that in the vitreous (2.6–4.0 days). Exposure to ranibizumab in the aqueous and the retina was 2- to 3.3-fold lower than in the vitreous, when comparing $AUC_{(0-\infty)}$. Figure 1C shows the ranibizumab concentrations in both retinal layers and in Ames solution after administration of 2000 μg/eye. Concentrations declined in parallel in both retinal layers and were approximately twofold greater in the NR than in the RPE/Bruch's. Ranibizumab concentrations also declined in parallel for the 500-μg/eye group (data not shown) and were approximately fourfold larger in the NR than in the RPE/Bruch's.

Ranibizumab Serum Pharmacokinetics after ITV and IV Administration

After ITV administration of 500 or 2000 μg/eye, ranibizumab serum t_{max} was 6 hours (Fig. 1) and declined thereafter. The $t_{½}$ was approximately 3.5 days, which is comparable to the $t_{½}$ in the ocular compartments (Table 4). Serum ranibizumab concentrations were low (Table 4): Group 1 and 2 serum C_{max} was 150 and 616 ng/mL, respectively. The overall ranibizumab concentration after ITV administration was >1500-fold lower than the corresponding vitreous concentration, based on $AUC_{(0-\infty)}$.

Ranibizumab serum PK in group-3 and -4 animals was analyzed after IV administration of identical total ranibizumab doses that were administered in groups 1 and 2 (i.e., 500 and 2000 μg/eye bilaterally equals 1000 and 4000 μg/animal, respectively). Clearance was approximately 40 mL/kg per hour. Ranibizumab terminal $t_{½}$ after IV administration was shorter than after ITV injection (14–15.5 hours versus 3.5–3.6 days; Table 5, Fig. 2). Bioavailability after ITV administration at 500 μg/eye and 2000 μg/eye was 50% and 60%, respectively.

Immunologic Response

No antibodies against ranibizumab were detected in the serum of any animals, indicating that ranibizumab was not immunogenic during the study period.

VEGF Ocular Concentrations

VEGF ocular $AUC_{(0-t)}$, after ITV administration of ranibizumab, are presented in Table 6 and Figure 3. Although retinal VEGF concentrations could not be determined at baseline, at both doses, VEGF concentrations did not change consistently after ranibizumab administration, suggesting no effect of the drug on VEGF. Vitreous VEGF concentrations were approximately 2.4- to 5.7-fold larger than in the aqueous, whereas retinal concentrations were approximately 2-fold greater than in the vitreous.

DISCUSSION

The objective of this study was to characterize the ranibizumab PK profile in monkeys, a drug in phase III clinical trials for the treatment of neovascular AMD (Heier JS. *IOVS* 2003;44:ARVO E-Abstract 972). Cynomolgus monkeys were selected, because this species was used to characterize the ranibizumab toxicology profile. To characterize ranibizumab concentrations in the vitreous and the retina, the animals could be sampled once only (as opposed to several samples/animal), and thus multiple animals were used. Our findings indicate that ranibizumab clears in parallel from all ocular compartments, with terminal $t_{½}$ of 3 days. Ranibizumab $t_{½}$ in the aqueous chamber and vitreous body was similar to the terminal $t_{½}$ in the rabbit vitreous body and aqueous chamber (2.1–3 days).[18] The impact of the mild ocular inflammation on ranibizumab disposition was not specifically addressed in the present study. However, in previous studies, when rabbits received 25 or 625 μg ranibizumab per eye, the terminal $t_{½}$ was similar in both groups, whereas more pronounced ocular inflammation was observed in the 625-μg/eye group, suggesting that inflammation did not significantly affect the clearance of ranibizumab from the vitreous.[18]

Downloaded from iovs.arvojournals.org on 01/21/2024

Regeneron Ex. 2017
Fresenius v. Regeneron
IPR2025-01268
Page 3 of 8

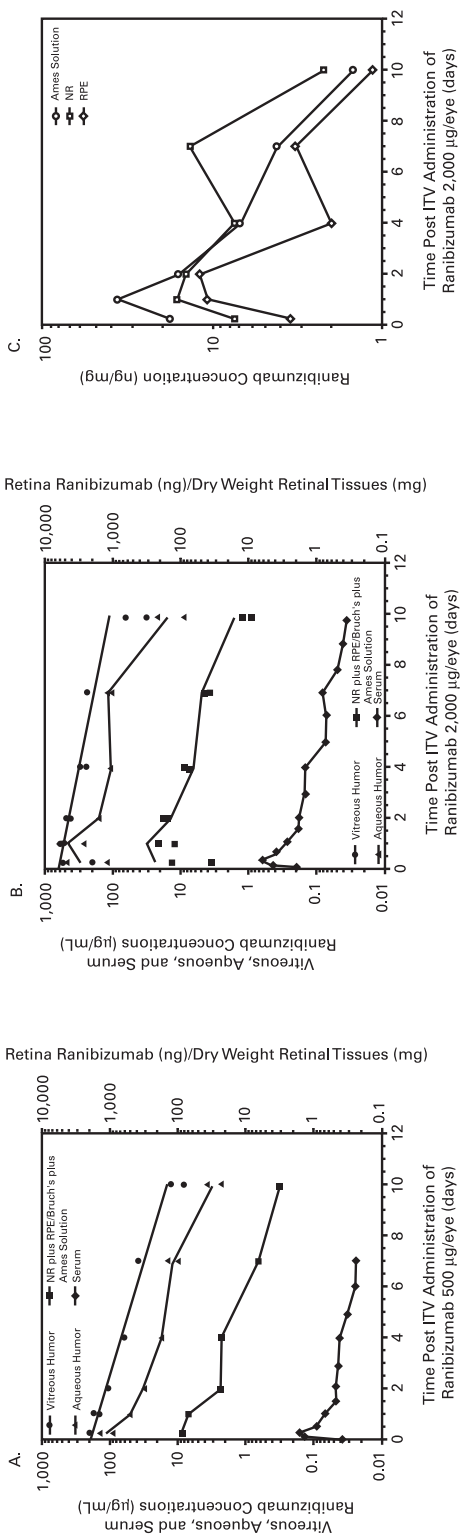

FIGURE 1. Individual ranibizumab concentration–time profiles for the vitreous humor, aqueous humor, retina, and serum after 500 (**A**) or 2000 (**B**) µg/eye ITV administration. The vitreous humor compartmental fit is superimposed on the observed data. (**C**) Mean ranibizumab concentration–time profiles for the NR, RPE, and Ames solution after ITV administration of 2000 µg/eye. NR, neural retina; RPE, retinal pigment epithelium.

TABLE 4. Ranibizumab Serum Pharmacokinetics after ITV Administration (Noncompartmental Model)

	Group 1 (500 µg/eye)	Group 2 (2000 µg/eye)
C_{max} (ng/mL)	150	616
t_{max} (d)	0.25	0.25
CL/F (mL/d)	2,310	2,760
Terminal $t_{½}$ (d)	3.59	3.47
MRT (d)	5.19	4.48
$AUC_{(0-2d)}$ (d · ng/mL)	147	586
$AUC_{(0-t)}$ (d · ng/mL)	315	1270
$AUC_{(0-\infty)}$ (d · ng/mL)	433	1450

C_{max}, observed maximum concentration; t_{max}, time to C_{max}; CL, clearance; F, bioavailability; MRT, mean residence time; $AUC_{(0-2d)}$, area under the curve up to 2 days; $AUC_{(0-t)}$, area under the curve until the last measurable concentration (~7 days); and $AUC_{(0-\infty)}$, area under the curve from 0 to infinity.

TABLE 5. Ranibizumab Serum Pharmacokinetics after IV Administration (Compartmental Model)

	Group 3 (1000 µg/animal)	Group 4 (4000 µg/animal)
Initial $t_{½}$ (h)	0.44 ± 0.068	0.45 ± 0.11
Terminal $t_{½}$ (h)	15.5 ± 11.5	14.0 ± 5.6
CL (mL/kg per h)	41.1 ± 6.3	46.0 ± 12.5
V_c (mL/kg)	43.0 ± 7.3	32.2 ± 3.2
V_{ss} (mL/kg)	431 ± 393	213 ± 111
MRT (h)	10.1 ± 9.6	6.0 ± 3.8
$AUC_{(0-t)}$ (day · ng/mL)*	246 ± 9.17	1,180 ± 276

CL, clearance; V_c, central volume of distribution; V_{ss}, volume of distribution at steady state; MRT, mean residence time; and $AUC_{(0-t)}$, area under the curve until the last measurable timepoint.

* $AUC_{(0-t)}$ is equivalent to $AUC_{(0-2d)}$.

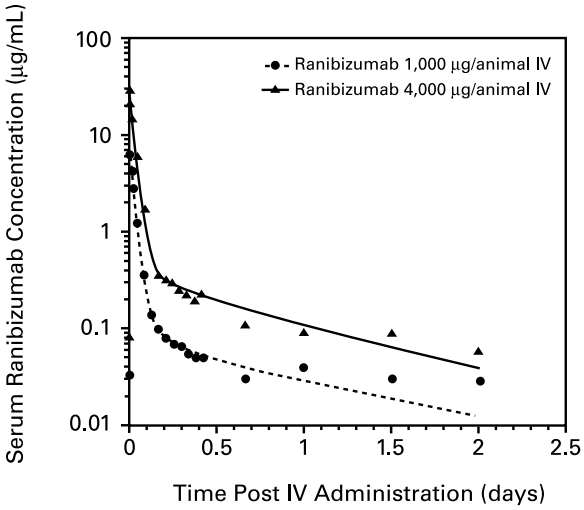

FIGURE 2. Mean ranibizumab concentration–time profile in serum after IV administration. A two-compartmental fit is superimposed on observed data.

Downloaded from iovs.arvojournals.org on 01/21/2024

Regeneron Ex. 2017
Fresenius v. Regeneron
IPR2025-01268
Page 4 of 8

Table 6. VEGF Ocular $AUC_{(0-t)}$ of Ranibizumab after ITV Administration

	Group 1 500 μg/eye (day · ng/mL)	Group 2 2000 μg/eye (day · ng/mL)
Vitreous humor	34.9	27.8
Aqueous humor	5.13	11.6
Retina	60.1	73

* $AUC_{(0-t)}$ is equivalent to $AUC_{(0-2d)}$.

Studies conducted in rabbits indicate that drug clearance from the vitreous depends on molecular size.[21] Small molecules, such as fluconazole and ciprofloxacin (<350 Da), have a terminal $t_{½}$ of 2 to 3 hours when administered ITV.[22,23] In contrast, the $t_{½}$ of albumin (67 kDa) is 4.3 days,[24] and the terminal $t_{½}$ of the full-length antibody trastuzumab (148 kDa) is 5.6 days.[25] Consistent with this principle, the vitreous $t_{½}$ of ranibizumab (48 kDa) was 2.6 to 4.0 days. Because the rate of intraocular drug loss appears to be partly controlled by diffusion, it is sensitive to ocular geometry.[21] Thus, species with bigger eyes and longer diffusion paths would be expected to have slower vitreous clearance. Other mechanisms, such as convection, may play a role in vitreous clearance; therefore, the $t_{½}$ of ranibizumab in humans is difficult to predict and may be longer than in animals, because the human eye is larger (human vitreous, 4.5 mL versus 1.5 mL in rabbits and monkeys).[26] However, data from clinical trials are needed to characterize the human $t_{½}$.

Ranibizumab distributed rapidly to the retina, and retinal concentrations were approximately one third of the vitreous

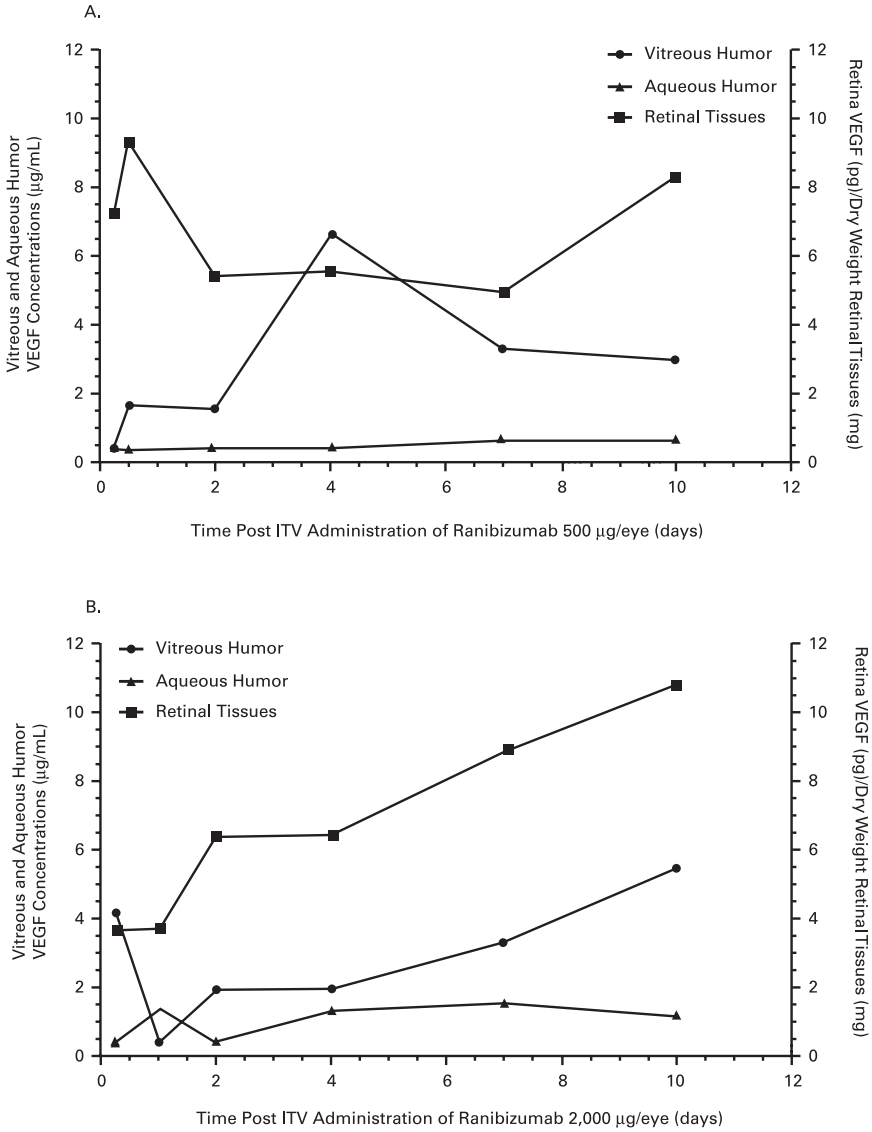

Figure 3. VEGF concentration–time profiles for the vitreous humor, aqueous humor, and retinal compartments after ITV injection of ranibizumab at 500 (**A**) or 2000 (**B**) μg/eye.

Downloaded from iovs.arvojournals.org on 01/21/2024

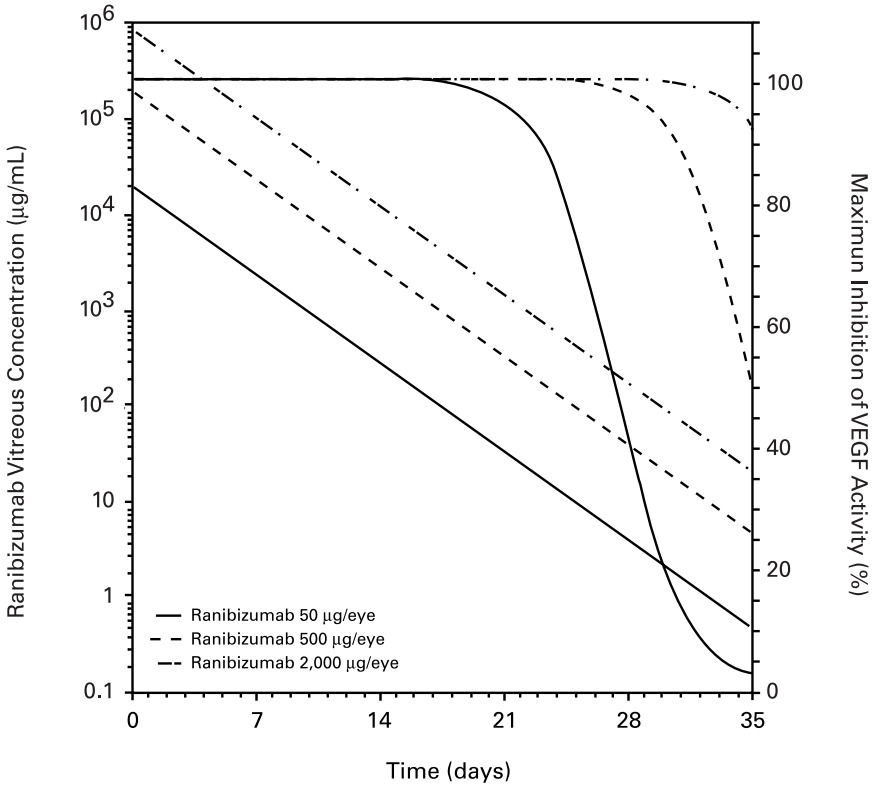

FIGURE 4. Predicted concentration–effect on VEGF activity after ITV administration of various doses of ranibizumab. The linear curves represent the predicted ranibizumab concentration in the vitreous humor, and the sigmoidal curves represent the time course of ranibizumab inhibition of VEGF, based on in vitro inhibition studies.

concentrations at both doses. The ability of ranibizumab to penetrate the retina in monkeys is consistent with previous observations in rabbits[18] and with those of a study investigating the ocular distribution of rhuFabV1, a first-generation anti-VEGF antibody fragment, in rhesus monkeys.[19] Notably, penetration of ranibizumab into the retina is critical for its clinical use. Retinal penetration suggests the availability of ranibizumab to inactivate VEGF at the site of AMD, leading to inhibition of CNV and vessel permeability reduction. In our study, the eyes were not immediately flash frozen after euthanasia. Therefore, ranibizumab may have redistributed between the retinal layers, which may affect its distribution. However, dissection was completed shortly after euthanasia, and the data in Figure 1C also suggest that redistribution did not play a significant role, because concentrations declined in parallel in all three matrices.

Experiments in rabbits showed the existence of two exit pathways for ranibizumab: one through the anterior chamber and aqueous drainage and the other through the retina.[18] In keeping with these findings, our study demonstrates the existence of an anterior exit pathway and supports the possibility of a retinal exit pathway, as ranibizumab was found in both retinal layers.

We also investigated the systemic bioavailability of ranibizumab after ITV administration. Fifty percent of the dose reached the circulation after 2 days, consistent with the vitreous $t_{½}$ of 3 days. These data suggest that intraocular metabolism does not play a significant role in elimination of ranibizumab from the vitreous. For most intraocularly administered drugs, the metabolic pathways remain unknown. To the best of our knowledge, the only drug for which ocular metabolism has been elucidated is fomivirsen, an antisense oligonucleotide metabolized by exonuclease digestion.[27]

The serum $t_{½}$ of ranibizumab after ITV and IV administration were also compared. Ranibizumab's terminal $t_{½}$ after ITV injection was 5.4- to 6.2-fold longer than after IV administration. The longer terminal $t_{½}$ after ITV administration most likely reflects the slow egress of drug from the eye into the serum, rather than the rate of elimination from the serum. Therefore, monitoring serum ranibizumab concentrations after ITV administration may provide insight into its ocular clearance.

Measurement of tissue ranibizumab concentrations after ITV administration was not a study objective, and the levels are unknown, because serum concentrations after ITV administration were low, and tissue concentrations would be too low for quantification by ELISA. The low circulating concentrations of ranibizumab after ITV administration may be important in the clinical setting, because VEGF is necessary for normal physiological functions such as tissue repair and reproduction.[20] Furthermore, VEGF is believed to be involved in attenuating ischemia in the brain, myocardium, and skeletal muscle,[28–30] maintenance of adequate VEGF systemic concentration is particularly important in the elderly, who constitute most of the AMD patient population. Notably, differences in the size of the serum compartments between monkeys and humans, lead to

Downloaded from iovs.arvojournals.org on 01/21/2024

Regeneron Ex. 2017
Fresenius v. Regeneron
IPR2025-01268
Page 6 of 8

different rates of elimination. This suggests that circulating exposure to ranibizumab in humans would be even lower than in monkeys and may reduce the likelihood of pharmacologic effects. This expectation is consistent with the initial trials investigating ITV administration of ranibizumab in patients with AMD, as serum ranibizumab concentrations were generally undetectable (sensitivity limit, 20 ng/mL) and systemic adverse events were rare (Heier JS. *IOVS* 2003;44:ARVO E-Abstract 972).[19]

After administration of ranibizumab, VEGF was detected in retinal layers and in the vitreous and aqueous humors (higher in the vitreous than in the aqueous humor). These findings are consistent with those reported for healthy human eyes, in which vitreous VEGF concentrations (8.8 ± 9.9 ng/mL) were consistently higher than in the aqueous humor (5.6 ± 9.9 ng/mL).[9] VEGF was also detected in the NR and the RPE/Bruch's layers, consistent with previous studies in healthy monkeys and in humans that demonstrated VEGF expression in the retina.[13,31] VEGF production has been found in several types of retinal cells, including the retinal vascular endothelial cells, pericytes, glial and RPE cells, and invasive leukocytes.[32–36] After administration of 500 μg/eye, retinal exposure to ranibizumab was >3000-fold larger than retinal exposure to VEGF, suggesting that this ranibizumab dose provides maximum inhibition of VEGF.

Ocular VEGF inhibition over time by ranibizumab ITV injection can be predicted using the inhibitory effect of ranibizumab on VEGF activity in a human umbilical vein endothelial cell assay,[37] and its ocular $t_{½}$ as determined in this study (Fig. 4). This prediction indicates that ranibizumab concentrations, capable of inhibiting VEGF in the eyes of patients with AMD, are expected to be achieved after ITV doses of 300 to 500 μg/mo.

In conclusion, after ITV administration of ranibizumab to monkeys, the concentration declined from all ocular compartments in parallel, with a relatively long terminal $t_{½}$ of 3 days. Serum concentrations after ITV administration of ranibizumab was >1000-fold lower than in the vitreous. Furthermore, the study indicates that ranibizumab distributes rapidly into the retina, with concentrations one third of those in the vitreous. The results of the present study, with those from earlier studies, provide the dosage rationale for the treatment of neovascular AMD with ITV ranibizumab.

References

1. Bressler NM, Bressler SB, Fine SL. Age-related macular degeneration. *Surv Ophthalmol*. 1988;32:375–413.
2. Leibowitz HM, Krueger DE, Maunder LR, et al. The Framingham Eye Study monograph: an ophthalmological and epidemiological study of cataract, glaucoma, diabetic retinopathy, macular degeneration, and visual acuity in a general population of 2631 adults, 1973–1975. *Surv Ophthalmol*. 1980;24:335–610.
3. D'Amico DJ. Diseases of the retina. *N Engl J Med*. 1994;331:95–106.
4. Tolentino MJ, Miller JW, Gragoudas ES, et al. Vascular endothelial growth factor is sufficient to produce iris neovascularization and neovascular glaucoma in a nonhuman primate. *Arch Ophthalmol*. 1996;114:964–970.
5. Kvanta A, Algvere PV, Berglin L, Seregard S. Subfoveal fibrovascular membranes in age-related macular degeneration express vascular endothelial growth factor. *Invest Ophthalmol Vis Sci*. 1996;37:1929–1934.
6. Lopez PF, Sippy BD, Lambert HM, Thach AB, Hinton DR. Transdifferentiated retinal pigment epithelial cells are immunoreactive for vascular endothelial growth factor in surgically excised age-related macular degeneration-related choroidal neovascular membranes. *Invest Ophthalmol Vis Sci*. 1996;37:855–868.
7. Krzystolik MG, Afshari MA, Adamis AP, et al. Prevention of experimental choroidal neovascularization with intravitreal anti-vascular endothelial growth factor antibody fragment. *Arch Ophthalmol*. 2002;120:338–346.
8. Adamis AP, Miller JW, Bernal MT, et al. Increased vascular endothelial growth factor levels in the vitreous of eyes with proliferative diabetic retinopathy. *Am J Ophthalmol*. 1994;118:445–450.
9. Aiello LP, Avery RL, Arrigg PG, et al. Vascular endothelial growth factor in ocular fluid of patients with diabetic retinopathy and other retinal disorders. *N Engl J Med*. 1994;331:1480–1487.
10. Malecaze F, Clamens S, Simorre-Pinatel V, et al. Detection of vascular endothelial growth factor messenger RNA and vascular endothelial growth factor-like activity in proliferative diabetic retinopathy. *Arch Ophthalmol*. 1994;112:1476–1482.
11. Pe'er J, Shweiki D, Itin A, et al. Hypoxia-induced expression of vascular endothelial growth factor by retinal cells is a common factor in neovascularizing ocular diseases. *Lab Invest*. 1995;72:638–645.
12. Robinson CJ, Stringer SE. The splice variants of vascular endothelial growth factor (VEGF) and their receptors. *J Cell Sci*. 2001;114:853–865.
13. Kim I, Ryan AM, Rohan R, et al. Constitutive expression of VEGF, VEGFR-1, and VEGFR-2 in normal eyes. *Invest Ophthalmol Vis Sci*. 1999;40:2115–2121.
14. Gerhardinger C, Brown LF, Roy S, et al. Expression of vascular endothelial growth factor in the human retina and in nonproliferative diabetic retinopathy. *Am J Pathol*. 1998;152:1453–1462.
15. Shima DT, Adamis AP, Ferrara N, et al. Hypoxic induction of endothelial cell growth factors in retinal cells: identification and characterization of vascular endothelial growth factor (VEGF) as the mitogen. *Mol Med*. 1995;1:182–193.
16. Shima DT, Gougos A, Miller JW, et al. Cloning and mRNA expression of vascular endothelial growth factor in ischemic retinas of *Macaca fascicularis*. *Invest Ophthalmol Vis Sci*. 1996;37:1334–1340.
17. Stump DC, Mann KG. Mechanisms of thrombus formation and lysis. *Ann Emerg Med*. 1988;17:1138–1147.
18. Gaudreault J, Webb W, Van Hoy M, et al. Pharmacokinetics and retinal distribution of AMD rhufab V2 after intravitreal administration in rabbits. *AAPS Pharm Sci*. 1999;(suppl 1):3207.
19. Mordenti J, Cuthbertson RA, Ferrara N, et al. Comparisons of the intraocular tissue distribution, pharmacokinetics, and safety of 125I-labeled full-length and Fab antibodies in rhesus monkeys following intravitreal administration. *Toxicol Pathol*. 1999;27:536–544.
20. Ferrara N, Davis-Smyth T. The biology of vascular endothelial growth factor. *Endocr Rev*. 1997;18:4–25.
21. Maurice DM, Mishima S. Ocular pharmacokinetics. In: Sears M, ed. *Pharmacology of the Eye*. Berlin: Springer-Verlag; 1984:19–116.
22. Gupta SK, Velpandian T, Dhingra N, Jaiswal J. Intravitreal pharmacokinetics of plain and liposome-entrapped fluconazole in rabbit eyes. *J Ocul Pharmacol Ther*. 2000;16:511–518.
23. Pearson PA, Hainsworth DP, Ashton P. Clearance and distribution of ciprofloxacin after intravitreal injection. *Retina*. 1993;13:326–330.
24. Maurice D. Protein dynamics in the eye studies with labeled proteins. *Am J Ophthalmol*. 1959;47:361–367.
25. Mordenti J, Thomsen K, Licko V, et al. Intraocular pharmacokinetics and safety of a humanized monoclonal antibody in rabbits after intravitreal administration of a solution or a PLGA microsphere formulation. *Toxicol Sci*. 1999;52:101–106.
26. Maurice DM. Injection of drugs into the vitreous body. In: Leopold I, Burns R, ed. *Symposium on Ocular Therapy*. New York: John Wiley & Sons; 1976:59–72.
27. Leeds JM, Henry SP, Bistner S, et al. Pharmacokinetics of an antisense oligonucleotide injected intravitreally in monkeys. *Drug Metab Dispos*. 1998;26:670–675.
28. Brizzi MF, Formato L, Bonamini R. The molecular mechanisms of angiogenesis: a new approach to cardiovascular diseases. *Ital Heart J*. 2001;2:81–92.
29. Croll SD, Wiegand SJ. Vascular growth factors in cerebral ischemia. *Mol Neurobiol*. 2001;23:121–135.

Downloaded from iovs.arvojournals.org on 01/21/2024

30. Miraliakbari R, Francalancia NA, Lust RM, et al. Differences in myocardial and peripheral VEGF and KDR levels after acute ischemia. *Ann Thorac Surg*. 2000;69:1750–1753.
31. Kliffen M, Sharma HS, Mooy CM, Kerkvliet S, de Jong PT. Increased expression of angiogenic growth factors in age-related maculopathy. *Br J Ophthalmol*. 1997;81:154–162.
32. Yoshida A, Yoshida S, Ishibashi T, Inomata H. Intraocular neovascularization. *Histol Histopathol*. 1999;14:1287–1294.
33. Lutty GA, McLeod DS, Merges C, Diggs A, Plouet J. Localization of vascular endothelial growth factor in human retina and choroid. *Arch Ophthalmol*. 1996;114:971–977.
34. Adamis AP, Shima DT, Yeo KT, et al. Synthesis and secretion of vascular permeability factor/vascular endothelial growth factor by human retinal pigment epithelial cells. *Biochem Biophys Res Commun*. 1993;193:631–638.
35. Nomura M, Yamagishi S, Harada S, et al. Possible participation of autocrine and paracrine vascular endothelial growth factors in hypoxia-induced proliferation of endothelial cells and pericytes. *J Biol Chem*. 1995;270:28316–28324.
36. Aiello LP, Northrup JM, Keyt BA, Takagi H, Iwamoto MA. Hypoxic regulation of vascular endothelial growth factor in retinal cells. *Arch Ophthalmol*. 1995;113:1538–1544.
37. Chen Y, Wiesmann C, Fuh G, et al. Selection and analysis of an optimized anti-VEGF antibody: crystal structure of an affinity-matured Fab in complex with antigen. *J Mol Biol*. 1999;293:865–881.

Downloaded from iovs.arvojournals.org on 01/21/2024